Advances in Bamboo Science 9 (2024) 100115

Contents lists available at ScienceDirect

Advances in Bamboo Science

journal homepage: www.journals.elsevier.com/advances-in-bamboo-science

Moisture ageing effects on the mechanical performance of eco-friendly sandwich panels made of aluminium skins, bamboo ring core and bio-based adhesives

Flávio Napolitano [a], Júlio Cesar dos Santos [a,b], Rodrigo José da Silva [a,c], Guilherme Germano Braga [a], José Ricardo Tarpani [b], Túlio Hallak Panzera [a,*], Fabrizio Scarpa [c]

[a] Centre for Innovation and Technology in Composite Materials (CITeC), Federal University of São João del-Rei (UFSJ), São João del-Rei, Brazil
[b] São Carlos School of Engineering (EESC), University of São Paulo (USP), São Carlos, Brazil
[c] Bristol Composites Institute (ACCIS), University of Bristol, Bristol, United Kingdom

ARTICLE INFO

Keywords:
Sandwich panel
Sustainable structure
Bamboo
Mechanical properties
Ageing effect

ABSTRACT

Recent research has been focused on developing high-performance sandwich structures using renewable resources. The adoption of bamboo rings as a core material and bio-based adhesives has emerged as a promising sustainable design solution for panel construction. It is therefore critical to conduct accelerated ageing tests on these materials to evaluate the impact of environmental humidity on their degradation and durability. This study assessed the effects of moisture ageing on the physic-mechanical properties of eco-friendly sandwich panels and their constituents (aluminium skins, bamboo ring core and castor oil bio-adhesive). Mechanical evaluations of sandwich panels with compacted and spaced bamboo ring cores were performed under varying humidity conditions. Bamboo rings exhibited variable bulk density due to swelling and loss of organic material over time. They also demonstrated increased compressive properties after 2 years of natural ageing but reduced performance after 30 days at 100 % relative humidity. The mechanical properties of the bio-based polymer were enhanced through water-ageing exposure. Sandwich panels constructed with compacted bamboo ring cores exhibited higher bending properties than those with spaced ring core architecture, with the latter showing failures characterised by a wrinkling effect on both skins followed by debonding.

1. Introduction

Sandwich panels are lightweight structures consisting primarily of two skins (also referred to as faces or facesheets) and a low-density core, interconnected mechanically or through adhesion (Daniel and Ishai, 2005). With the use of diverse material types in the skins (Wang et al. 2019; Cai et al. 2020; Hartoni, et al. 2017; Waddar et al. 2019; Jen and Chang, 2009) and the core (Vieira et al. 2022), these structures exhibit significant flexural and impact resistance, making them suitable for a wide range of engineering applications. In the current global emphasis on environmentally friendly products, aluminium stands out as a prominent material due to its high recyclability, along with its established use in automotive (Bitzer, 1997) and aeronautical (Dursun and Soutis, 2014) applications due to its low density and corrosion resistance (Sheasby and Pinner, 2001). Consequently, research in various fields has focused on utilizing aluminium skins in the fabrication of high-performance sandwich structures (Sun et al. 2017; Oliveira et al. 2018; Jamil et al. 2019). Simultaneously, in pursuit of eco-friendly design, the use of bio-based adhesives for bonding panel skins and cores presents an attractive alternative to conventional petrochemical adhesives. These adhesives provide sufficient adhesion with minimal usage and serve as renewable options to replace synthetic adhesives (Pizzi and Mittal, 2003; Heinrich, 2019).

The use of tubular honeycombs as core material to enhance the mechanical performance of sandwich structures has been extensively studied, showcasing advantages over hexagonal honeycombs (Gotkhindi and Simha, 2015; Oruganti and Ghosh, 2008; Hu et al. 2015; Lin, Chen, and Huang, 2012; Chung and Waas, 2000; Cabrera et al. 2008). In line with the pursuit of innovative and sustainable products, Oliveira et al. (2017) demonstrated promising flexural properties in panels utilizing a core derived from disposable PET bottle caps and aluminium skins.

* Corresponding author.
E-mail address: panzera@ufsj.edu.br (T.H. Panzera).

https://doi.org/10.1016/j.bamboo.2024.100115
Received 20 June 2024; Received in revised form 16 October 2024; Accepted 17 October 2024
Available online 19 October 2024

Recent studies underscore the potential of wood-based materials and composites in advancing sustainable construction practices. Research highlights the advantages of wood and plywood in developing eco-friendly mobility solutions while exploring their structural capabilities in sandwich panel applications. The performance of these materials under various conditions is well-documented, demonstrating their strength and versatility. Furthermore, integrating wood with other engineering materials has been shown to enhance sustainability, providing promising alternatives for creating green building solutions (Wei et al. 2021; Oliveira et al.2022; Labans et al., (2017); Castanié et al. 2023). Furthermore, a sandwich structure integrating aluminium skins, bamboo ring core and castor oil bio-adhesive has emerged as a promising eco-friendly solution (de Oliveira et al. 2021).

Further evaluations are necessary for bio-based materials such as bamboo rings and castor oil-based adhesives. Conducting accelerated ageing tests on these materials is essential to assess their impact on mechanical performance. Accelerated ageing tests provide the advantage of speed, offering insights into the potential performance of the material over its expected lifespan. These tests simulate the exposure conditions of the material, but with high intensities, to accelerate the degradation process (Maria et al. 2007; Santos et al. 2020; Assarar et al., 2011; Regazzi et al. 2016).

In the context of accelerated ageing, environmental humidity plays a significant role. The hygroscopic nature of bamboo holds considerable importance for researchers exploring its applications. Authors (Yuan et al. 2021a) have emphasised the dimensional variations of bamboo due to the presence of moisture. Additionally, the size of bamboo fibres affects the moisture content, as indicated in Yuan et al. (2021b). Jia et al. (2023) investigated storage conditions under varying levels of relative humidity (45 %, 60 %, 75 %, and 95 %), highlighting humidity as a key factor influencing degradation by mould and impacting bamboo quality. Within the context of sandwich structures composed of bamboo rings and bio-based adhesives, the assessment of water ageing needs to be contextualized within the framework of both bio-based materials. This investigation should be conducted on each material separately and on the sandwich structure, as each constituent element of the structure may exhibit distinct behaviour in aggressive moisture environments.

This study is the first to evaluate the effects of water ageing on the three-point bending performance of eco-friendly sandwich panels composed of aluminium skins, a bamboo ring core and bio-based adhesives. The research also involved assessing the impact of humidity on the individual bio-based components through accelerated ageing. It included mechanical assessments of the adhesive and core materials in their pristine condition and after exposure to water ageing. The bamboo rings were subjected to compressive loads, while the castor-oil polymer samples underwent both tensile and compression tests. Furthermore, the bamboo rings were tested with and without treatment using a boric acid and copper sulphate solution to prevent mould or fungus growth and preserve their mechanical properties after exposure to water ageing.

Based on prior research (Napolitano et al. 2023), the sandwich panels were fabricated using treated bamboo rings arranged in a hexagonal packing, with both compacted and spaced configurations. The introduction of spacing between rings aimed to reduce the equivalent density and costs of the structures. The response variables included equivalent density and flexural properties, measured through three-point bending tests. For a proper understanding of the effect of the gaps among bamboo rings, the panel's dimensions were designed to induce significant shear stresses within the core during the elastic regime. Compared to the compacted core, the spaced bamboo ring core increased internal voids by approximately 40 %, leading to a 26 % reduction in equivalent density. The mechanical performance of spaced-core panels was generally reduced compared to their pristine condition, primarily due to high shear deformations. However, when structural dimensions were considered and shear deformations disregarded, the specific flexural modulus (rigidity) of spaced-ring panels increased by 37 % compared to their pristine condition. Given the potential design demand for greater specific flexural modulus in applications of sandwich panels in structural dimensions, it is important to investigate the effect of water ageing on spaced-ring panels. Additionally, it is worth noting that for certain applications that prioritize lightweight, cost-effectiveness and lower structural requirements, spaced-bamboo structures could serve as an alternative to the original panel.

In this work, a full factorial Design of Experiment (DoE) was employed, combining compacted and spaced core configurations, different environmental conditions (55 % and 100 % relative humidity), and ageing times of 8 and 30 days. The DoE method systematically evaluates individual effects and interactions through structured experimental plans, finding extensive applications in various fields, including the assessment of materials and structures in physical and mechanical domains (dos Santos et al. 2022; Vial et al. 2023; Kieling et al., 2023; Assis et al. 2023; Lopes et al. 2023; dos Santos et al. 2024).

2. Materials and methods

The sandwich structures utilised 0.4 mm thick aluminium sheets (3105-O) as facing materials. This type of aluminium typically contains approximately 0.3–0.6 % copper, 0.3–0.6 % manganese, and 0.4–0.7 % iron, with the remainder being aluminium. Bamboo rings were extracted from the mid-basal portion of 6-meter culms of *Bambusa tuldoides* Munro, harvested in Brazil at the geographical coordinates (−21.1408, −44.2616). This selected portion of the plant enabled the extraction of bamboo rings with a diameter of 30 mm and a height of 14 mm, as per previous reports (Napolitano et al. 2023). The adhesive phase consisted of a castor oil-based polyurethane polymer supplied by Imperveg company (Brazil), which is a bi-component resin comprising diisocyanate and a vegetal-based polyol.

The manufacturing of the sandwich structures followed the material selection and bamboo ring drying process protocols outlined in previous studies (Napolitano et al. 2023; Oliveira et al. 2021). The bamboo rings, collected from multiple stems, were chosen based on their external diameter, which for this research was approximately 30 mm. The selected culms were stored upright in an enclosed, ventilated environment for 30 days to ensure uniform drying and minimize the risk of deformations that can occur with horizontal storage. For comparative study purposes, the drying time adopted for bamboo was based on the experimental approaches of another publication (Oliveira et al., 2021). Following the drying period, the bamboo culms were cut using a bandsaw for subsequent analysis and the fabrication of the sandwich materials. Bamboo ring samples were stored in a ventilated, dry place, free from UV light, allowing only variations in ambient humidity to conduct annual compression tests. This experimental approach was conducted to evaluate the mechanical properties of bamboo under conditions simulating those of a core material. As a core, the rings are protected from water and UV radiation by the aluminum faces. The dimensions of the sandwich panels adhered to the guidelines of ASTM C393 (2020). The arrangement of the unit cells, as shown in Fig. 1a, featured samples measuring 240 mm×90 mm x 15 mm and 270 mm×95 mm x 15 mm.

Initially, the aluminium faces underwent an abrasion process with 80-grit sandpaper to enhance their contact area with the polyurethane resin. The bamboo rings were stacked according to the diagram depicted in Fig. 1a, utilising a hexagonal packing shape to improve the core material's mechanical shear properties, as evidenced in prior research (Gotkhindi and Simha, 2015; Oruganti and Ghosh, 2008; Hu et al. 2015; Lin, Chen, and Huang, 2012; Chung and Waas, 2000; Cabrera et al. 2008). To evaluate the effects of core ring spacing, a separation equivalent to half the radius distance (resulting in a 15-millimeter spacing between the edges of the rings in Fig. 1a) was chosen. Subsequently, the aluminium skin was positioned into a rectangular wood mould, and the bi-component resin, mixed in a ratio of 1:1.2 parts (diisocyanate: polyol), was applied to the aluminium faces to achieve an adherent layer

with a thickness of 1.5 mm. The layer thickness of 1.5 mm was determined based on the theoretical bulk volume calculated in SolidWorks®. This volume was then converted to mass using the bulk density of the castor-oil polymer system, which is 1.07 ± 0.05 g/cm^3. Following the deposition of bamboo rings under the fluid resin layer, the mould was closed, and a weight equivalent to 10 kg was placed atop the assembly, considering the resin gel time (approximately 6 hours) as shown in Fig. 1b. Subsequently, the consolidated skin and core were bonded to the second face using the same procedures employed for the initial aluminium face, as depicted in Fig. 1c. After 6 hours of gel time for the adhesive layer of the second skin, the approximately 15 mm thick sandwich panels were left for complete curing over 14 days under controlled conditions of 23ºC temperature and 55 % relative humidity, as shown in Fig. 1d. The curing time was determined by the manufacturer of the castor-oil-based resin (Imperveg, Brazil).

2.1. Accelerate humidity ageing chambers

A humidity-controlled chamber (Equilam) was used to maintain a constant temperature at 25°C (±2°C) and 100 % relative humidity (RH). Reference samples with controlled temperature and relative humidity were set at 25°C (±2°C) and 55 % (±5 %) RH levels, respectively. The ageing process encompassed individual components and the sandwich structure itself. The dimensions of the samples used in the chamber were determined based on the mechanical characterisation step, which will be elaborated upon further.

2.2. Bamboo natural and accelerated ageing by humidity

The bamboo samples were cut into standardised dimensions for compression tests, with the height-to-diameter ratio set at H = 2*D. Following the cutting process, the samples were subjected to a 30-day drying period, during which they were kept upright to prevent distortions, cracks or deformations. Analyses were conducted at various intervals, including the initial reference (Ref.), 1 year later, and 2 years later, all at room temperature (R.T.). The mean relative humidity in São João del Rei city, Brazil, ranges from 62 % to 80 %, while the mean temperature ranges from 21.9 to 26 °C throughout the year (Climate Data website, 2024). Additionally, evaluations were performed at 8-day and 30-day intervals under 100 % RH. Table 1 illustrates the experimental variation adopted for the compression analysis. The samples exposed to ambient temperature conditions underwent variations influenced by climate-related humidity. These conditions were carefully controlled to isolate the influence of temperature and humidity, protecting the samples from the effects of rain and weathering. Fig. 2 depicts the samples prepared for the test (item a) and the ageing process under 100 % relative humidity (item b). For each experimental evaluation, ten samples were randomly selected. To assess the bulk density of bamboo samples under varying environmental and humidity conditions, each sample was accurately weighed in both its dry and conditioned states, while its volume was measured through geometric calculations based on instant measurements. The volume of the bamboo rings was determined by measuring the outer and inner diameters, as well as the height of each ring. The volume of the bamboo ring was then calculated

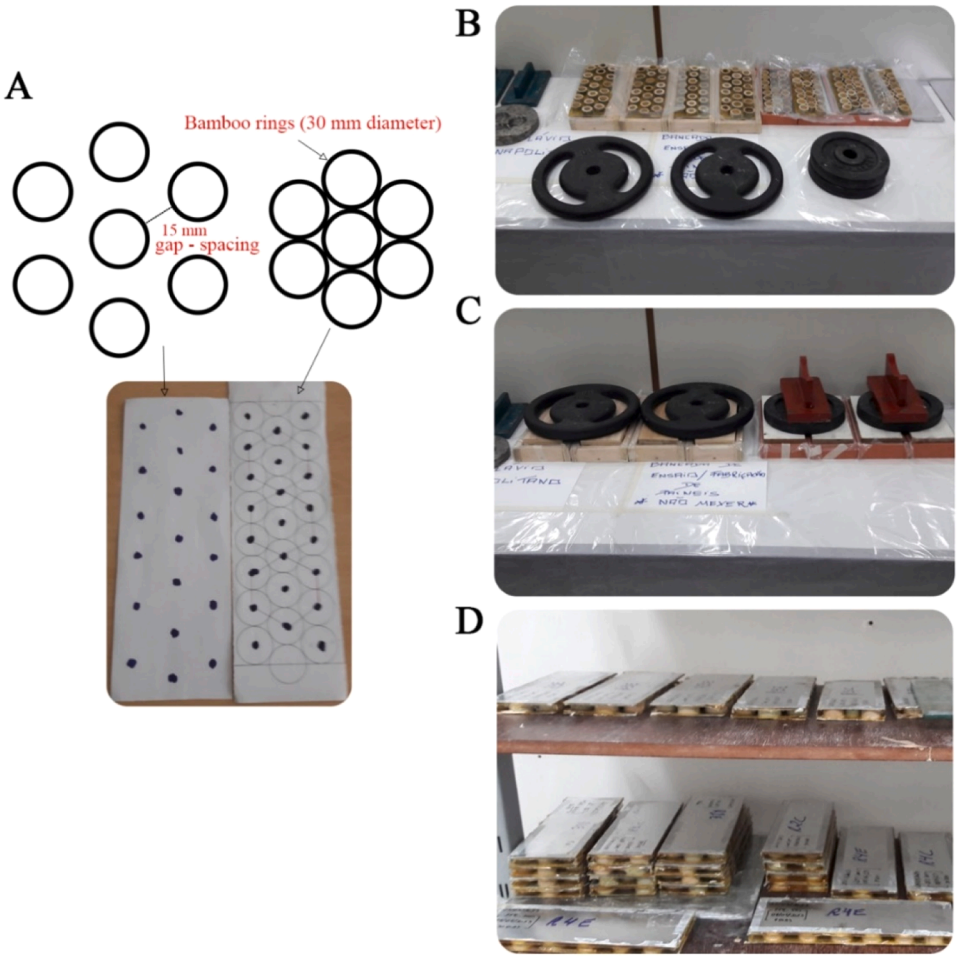

Fig. 1. Manufacturing process: (a) core packing configurations and template used, (b) first side aluminium bonded, (c) two faces sandwich assembled left to complete cure time, and (d) samples for bending tests.

by subtracting the volume of the inner cylinder from that of the outer cylinder. Finally, the bulk density was calculated by dividing the mass by its respective volume.

2.3. Castor-oil-based polyurethane accelerated ageing by humidity

Silicone moulds (Fig. 2c) were used to produce polymer samples following ASTM standards for tension and compression testing. The castor-oil polyurethane (PU), a bi-component polymer system provided by Imperveg Company (Brazil), was obtained by blending a diisocyanate-based hardener (component A) with a polyol (component B) in a mass mixing ratio of 1:1.2 (A:B). The liquid mixture was poured into the moulds and required a curing and post-curing period of 14 days before testing. Following the 14 days, the samples were removed from the silicone mould and reference conditions were maintained at room temperature (20–25°C), while the remaining samples were exposed to 100 % RH for 8 and 30 days (as shown in Fig. 2d). Each experimental condition involved testing five (5) samples, as detailed in Table 2.

2.4. Physical and mechanical testing

The characterisation of bamboo rings under compression and aluminium alloy sheets (3105-O) under tension was performed using a Shimadzu AGX-Plus machine equipped with a 100 kN load cell. Additionally, the polyurethane polymer was characterised in tension and compression using an Instron machine equipped with 1 kN and 50 kN load cells, respectively, while the sandwich structures were tested under three-point bending using a 50 kN load cell. The tensile testing of aluminium, tensile and compression testing of PU polymer, and flexural shear testing of sandwich panels followed the protocols of ASTM standards ASTM E8/E8M-15a (2015), D 638 -15 (2015), D695 – 15 (2015), and C393 (2020), respectively. Mechanical extensometers were employed for all tensile tests. The crosshead displacement was utilised for the flexural shear test, with the span length calculated as 10 times the sandwich thickness. Additionally, the load and cleaver supports featured a bending radius of 3.5 mm.

2.5. Statistical analysis

The data were analysed using statistical methods (one-way Analysis of Variance - ANOVA and Design of Experiments - DoE) to discern the effects of the main factors and their interactions. Minitab software was used to analyse the data and create the statistical graphs. A confidence level of 0.05 was considered for this work, and the validation of the statistical methods incorporated the examination of R^2(adj) results to assess the data against the proposed model, along with the Anderson-Darling test for normality (P-Value $^{AD} \geq 0.05$) and the Bartlett and Levene tests for homogeneity (P-Value$^{BvL} \geq 0.05$), which are prerequisites for using ANOVA. The significance of the factors are identified if P-values are equal to or lower than 0.05, indicating differences between the means of the analysed responses. However, P-values above 0.05 indicate insufficient statistical evidence to reject the null hypotheses of normality and homogeneity. This suggests that the data likely follow a normal distribution and exhibits homogeneous variances, thereby validating the use of ANOVA. Additionally, Tukey's test was employed to identify conditions that differ from others, i.e., when they do not share a grouping letter (dos Santos et al. 2024).

ANOVA was utilised to investigate the impact of natural and accelerated ageing on bamboo rings and castor oil PU in a humidity chamber. Furthermore, a full factorial 2^2 Design of Experiment (DoE) was executed to evaluate the influence of the presence of spacing among rings in the core (non-spaced and spaced rings) and the ageing conditions (25 °C/100 % RH and 25 °C/55 % RH) on the mechanical responses of the sandwich structures (refer to Fig. 2d). Four experimental conditions, each involving five samples, were tested. Table 3 provides a summary of the statistical planning, including the response variables that were analysed.

Table 1
Experimental conditions for bamboo rings.

Setup	Condition	
	Temperature	% RH
Reference (Ref.)	R.T.	62–80
1-year	R.T.	62–80
2-years	R.T.	62–80
8-days	Chamber (Equilam)	100
30-days	Chamber (Equilam)	100

3. Results and discussions

3.1. Bulk density - Bamboo

The bulk density measurements are presented in Table 4. ANOVA results (Fig. 3) with P-values lower than or equal to 0.05 indicate the presence of at least one mean difference between the experimental conditions. Exposure to 100 % humidity for eight (8) days without treatment resulted in a 48 % increase in bamboo density. However, untreated samples exposed for 30 days experienced a 47.4 % reduction in density compared to the 8-day period, corresponding to a 22 % decrease from the original density (Ref.). The density notably increased during the initial 8 days due to water adsorption-induced swelling, which could be considered a temporary density increase (Yuan et al. 2021b). Subsequently, from 8 days up to 30, the elevated humidity likely created favourable conditions for microbial activity, initiating the decomposition of organic compounds. Prolonged exposure to water might induce internal chemical changes in bamboo fibres, leading to the rupture of chemical bonds or alterations in the molecular orientation of the fibres and a more parenchyma-relaxed structure (Yuan et al. 2021b). Moreover, a sudden loss of organic material can lead to a decrease in bamboo density. Fig. 4 depicts the treated (a,c) and untreated (b,d) bamboo specimens following 8 days (a-b) and 30 days (c-d) of exposure to 100 % relative humidity (RH). The untreated samples exhibited a noticeable green liquid, indicating the release of organic materials and the presence of mould (Fig. 4b,d).

3.2. Mechanical properties - Bamboo

Table 5 illustrates the compressive properties of the bamboo rings. Frequency histograms, encompassing compressive modulus and strength, were plotted to provide a comprehensive understanding of the natural variability of mechanical properties (Fig. 5a-d). Over the span from the first to the second year, the mechanical properties exhibited increases of 84–191 % for modulus and 15–96 % for strength, respectively. Bamboo demonstrates high sensitivity to seasonal changes in humidity, which contribute to gradual strengthening, and over time, chemical changes in the bamboo fibres lead to increased lignification (Yuan et al. 2021a). Conversely, the residual moisture content in bamboo rings may enhance their ductility, potentially reducing their compressive strength (Jakovljević et al., 2017). This inprovement in mechanical properties, observed after storing bamboo rings in a relative humidity (RH) environment of 62% to 80% for 1 to 2 years, may be due to insufficient drying of the rings before testing and prior to prolonged exposure in a humid environment. Under these conditions (62 to 80% RH), bamboo may experience gradual drying, leading to enhanced mechanical properties as the moisture content decreases over time. Future research should ensure that bamboo rings are thoroughly dried before testing under reference conditions and prior to storage for ageing in environments with 62 to 80% RH for 1 to 2 years.

After 30 days at 100 % relative humidity, the mechanical properties of the untreated bamboo exhibited considerable reductions (Table 5), with decreases of up to 78 % in both modulus and strength. No significant difference in compressive modulus was observed for bamboo

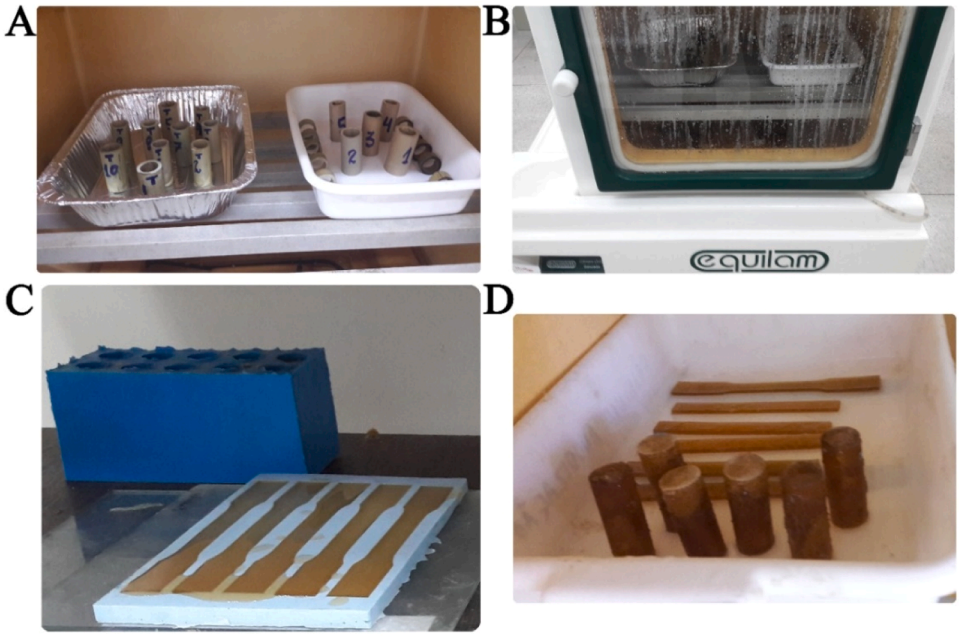

Fig. 2. Bamboo samples: (a) cuts with h=2*d; (b) under 100 % humidity in the Equilam chamber; (c) silicone compressive and tensile moulds; (d) polymers after 30 days of saturation in 100 % RH.

Table 2
Experimental conditions for castor oil PU.

Setup	Time (days)
Reference	0
8-d	8
30-d	30

exposed to a humidifying chamber from 8 to 30 days, since all share Group B (Table 5). The application of a treatment with boric acid and copper sulphate was ineffective in mitigating the impact of the aggressive moisture system (Fig. 4a), offering only marginal probabilities associated with the prevention of bacterial and fungicidal proliferation (Fig. 4b). The Tukey test (Table 5) also indicates that the compressive strength for both untreated and treated (T) conditions at 30 days was statistically equivalent to Group C, while the 8-day condition was categorized under Group B, followed by the reference (Group A) achieving the highest strength. The following paragraph explores the impact of humidity exposure on the weakening of bamboo.

Yuan et al. (2021b) provided significant insights into the weakening mechanism that governs the mechanical properties of bamboo under 100 % humidity conditions. When exposed to elevated humidity levels, water-layer molecules are absorbed from the external environment through adsorption, diffusing between the single molecular layer. Beyond 40 % RH, the monolayer moisture content reaches saturation, and water and lignin combine to form monolayer-absorbed water. The progressive increase in humidity leads to the formation of new H_2O-H_2O hydrogen bonds, which disrupt the original hydrogen bonds between native bamboo macromolecules, ultimately contributing to the initial stage of degradation of the material's mechanical properties. Furthermore, as indicated by the same authors, when the relative humidity (RH) exceeds 60 %, the cell wall of the fibres undergoes an increase in thickness and density, while the parenchyma experiences a decrease in thickness and a more relaxed structure. The swelling of both fibres and parenchyma, in both transverse and longitudinal directions, can lead to an increase and alterations in molecular orientation in the microfibril angle within the bamboo rings (Yuan et al. 2021b). The change in the microfibrillar angle can directly impact the mechanical properties of fibro-cellular materials, such as the reduction in compressive strength of bamboo due to the loss of organic material.

Table 3
Statistical planning.

Material	Factors	Responses	Statistical method
Bamboo	*Exposure Time:* ▪ Reference (R. T., 62–80 % RH) ▪ 1 year (R.T., 62–80 % RH) ▪ 2 years (R.T., 62–80 % RH) ▪ 8 days (100 % RH) ▪ 30 days (100 % RH)	Compressive modulus and strength	ANOVA One-Way
Castor-oil PU	*Exposure Time:* ▪ Reference (R. T., 62–80 % RH) ▪ 8 days (100 % RH) ▪ 30 days (100 % RH)	Compressive, tensile modulus and strength	ANOVA One-Way
Sandwich structure	*Core spacing:* ▪ Non-spaced ▪ Spaced rings Humidity: ▪ 25°C - 55 % RH ▪ 25°C - 100 % RH	Flexural, shear modulus and strength & Shear rigidity contribution*	DoE

3.3. Castor-oil polymer mechanical properties

Table 6 presents the descriptive statistics and ANOVA for castor oil polymers evaluated under 100 % RH. The tensile and compressive

Table 4
Bulk density properties of bamboo under 100 % RH.

E.C	Ref.	Treated		Untreated		ANOVA
		8 days	30 days	8 days	30 days	*p*-value
Bulk density (g/cm^3)	1.29 ± 0.1	1.64 ± 0.2	1.03 ± 0.04	1.92 ± 0.2	1.01 ± 0.3	*0.000*
Tukey test	BC	AB	C	A	C	R^2(adj) 78.32 %
Anderson Darling: 0.921 and Levene: 0.304						

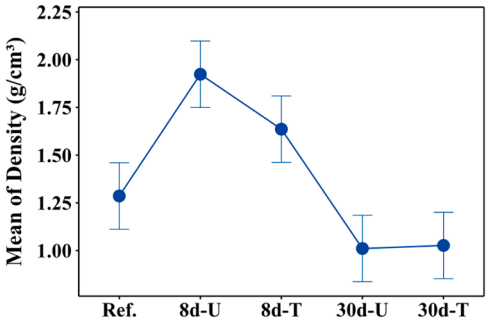

Fig. 3. ANOVA results for mean bulk density for untreated (U) and treated (T) bamboo samples.

Table 5
Mean values and ANOVA for compressive mechanical properties of bamboo rings.

Testing		Modulus	Strength	*Tukey-test grouping*	
		GPa	MPa	Modulus	Strength
Time factor at R.T.	Ref.	5.7 ± 2	76.0 ± 19	C	B
	1 year	10.5 ± 2	87.7 ± 10	B	B
	2 years	16.6 ± 4	149.2 ± 24	A	A
ANOVA	*p*-value	*0.000*	*0.000*		
	$R^2_{(adj)}$	78.49 %	76.21 %		
	A.D	0.547	0.598		
	Levene	0.689	0.054		
Humidifying chamber (100 % RH)	Ref.	12.6 ± 1	132.7 ± 14	A	A
	8-days	4.8 ± 2	52.8 ± 5	B	B
	T.8-days	5.0 ± 2	55 3 ± 6	B	B
	30-days	2.8 ± 0.5	29.1 ± 6	B	C
	T.30-days	3.1 ± 0.8	34 ± 3	B	C
ANOVA	*p*-value	*0.000*	*0.000*		
	$R^2_{(adj)}$	88.75 %	93.26 %		
	A.D	0.198	0.119		
	Levene	0.428	0.210		

Fig. 4. Treated (a) and untreated (b) bamboo rings after 8 days; and treated (c) and untreated (d) samples after 30 days of ageing in 100 % RH.

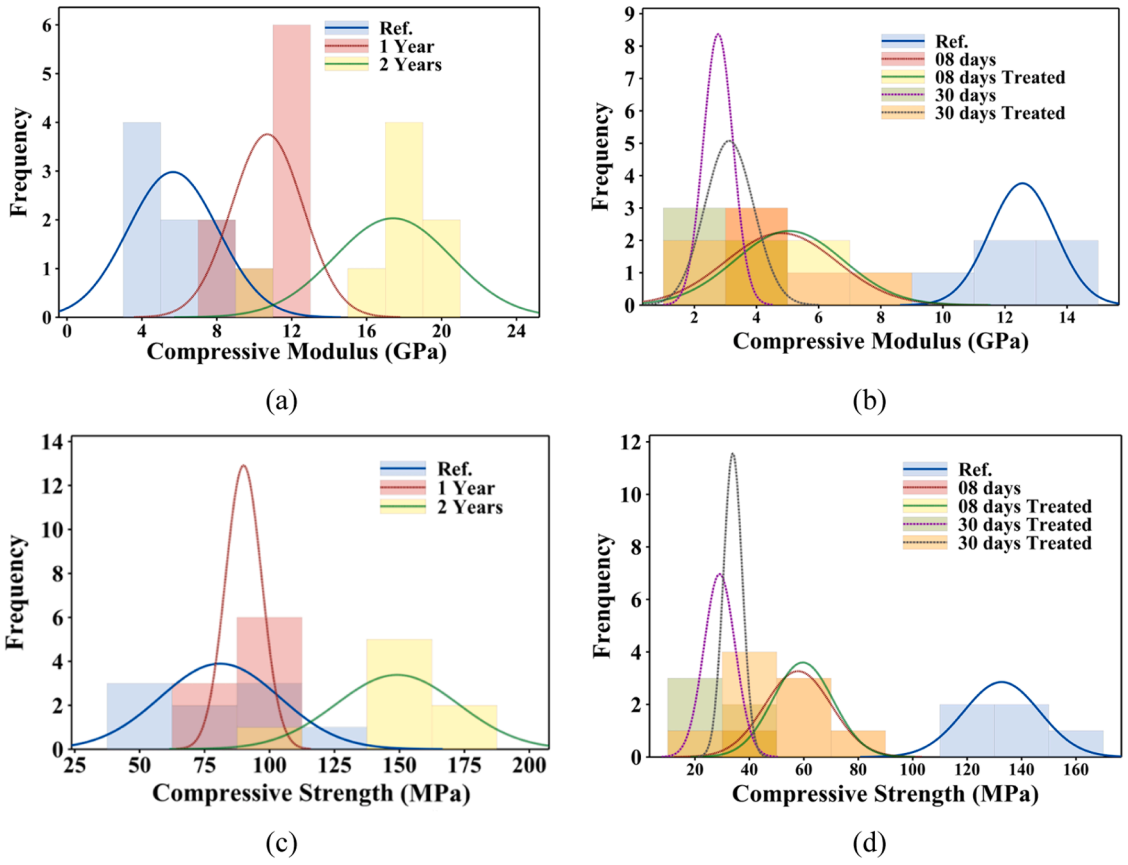

Fig. 5. Histogram graphs for compressive mechanical tests (a,c) yearly at R.T. and (b,c) humidifying chamber for modulus and strength.

properties exhibit increase correlated with the exposure time. Fig. 6a-d illustrate the variation of mean compressive properties, demonstrating significant increases in both elastic modulus (+261 %) and strength (+373 %) after 30 days of ageing. Tensile properties display less sensitivity to humidity variations, with a 38.5 % increase in elastic modulus and no significant change in strength. Water is considered a crosslinking agent for castor oil PU due to its interaction with isocyanate groups within the polyurethane formulation. This interaction initiates isocyanate trimerization, leading to the formation of urea linkages that enhance the polymer matrix through cross-linking (dos Santos et al. 2024; Szycher, 2012). Consequently, this process notably enhances the structural integrity, mechanical properties, and dimensional resilience of the biobased polyurethane (Napolitano et al. 2023).

3.4. Mechanical properties of the sandwich panels

Table 7 presents the mean bending properties of the sandwich panels under various ageing conditions. Table 8 provides the statistical analysis of the data based on a multilevel factorial design (DoE). The P-values for the main factors – core configuration (P-Value $^{\text{core conf.}}$), time exposure (P-Value $^{\text{Time exp.}}$) and % relative humidity (P-Value $^{\%RH}$) – are highlighted in bold to indicate significant effects. The interactions among the three main factors (P-Value $^{\text{3way-Int.}}$) reveal that only the flexural and core Shear modulus were not statistically significant. In summary, the three factors did not produce a relevant interaction that affected these response variables.

Notably, sandwich panels consisting of hexagonally compacted bamboo cores exhibited exceptional mechanical properties, as illustrated in Fig. 7. The highest maximum load was attained when the panels were constructed with compacted bamboo cores exposed to reduced time (8 days) and humidity (50 %) levels, as evidenced in Fig. 6a. Importantly, the decrease in load-carrying capacity after 30 days of ageing should not be viewed in isolation, but rather because of a complex interaction with the humidity variable, as depicted in Fig. 6b. The significant decline in maximum load at 100 % RH indicates that prolonged exposure to aggressive environments substantially diminishes the load-bearing capacity of these structures. Conversely, the interaction effect plot between relative humidity and exposure time (Fig. 6b) revealed no variation in maximum load at the lower level (50 % RH) of humidity.

Table 6
Mechanical properties of castor oil polymer under 100 % RH.

E.C.	Modulus (MPa)				Strength (MPa)			
	Tensile	Tukey	Compr.	Tukey	Tensile	Tukey	Compr.	Tukey
Ref.	51.4 ± 3	B	40.9 ± 6	C	10.0 ± 0.3	-	1.7 ± 0.3	C
8 days	67.9 ± 5	A	70.6 ± 4	B	10.4 ± 0.6	-	3.3 ± 0.2	B
30 days	71.1 ± 5	A	148.0 ± 9	A	11.6 ± 1	-	8.3 ± 0.5	A
ANOVA	*0.000*		*0.000*		0.067		*0.000*	
$R^2_{(adj)}$	77.74 %		97.95 %		37.67 %		74.30 %	
A.D	0.218		0.979		0.070		0.192*	

* Johnson is used to obtain normal distribution

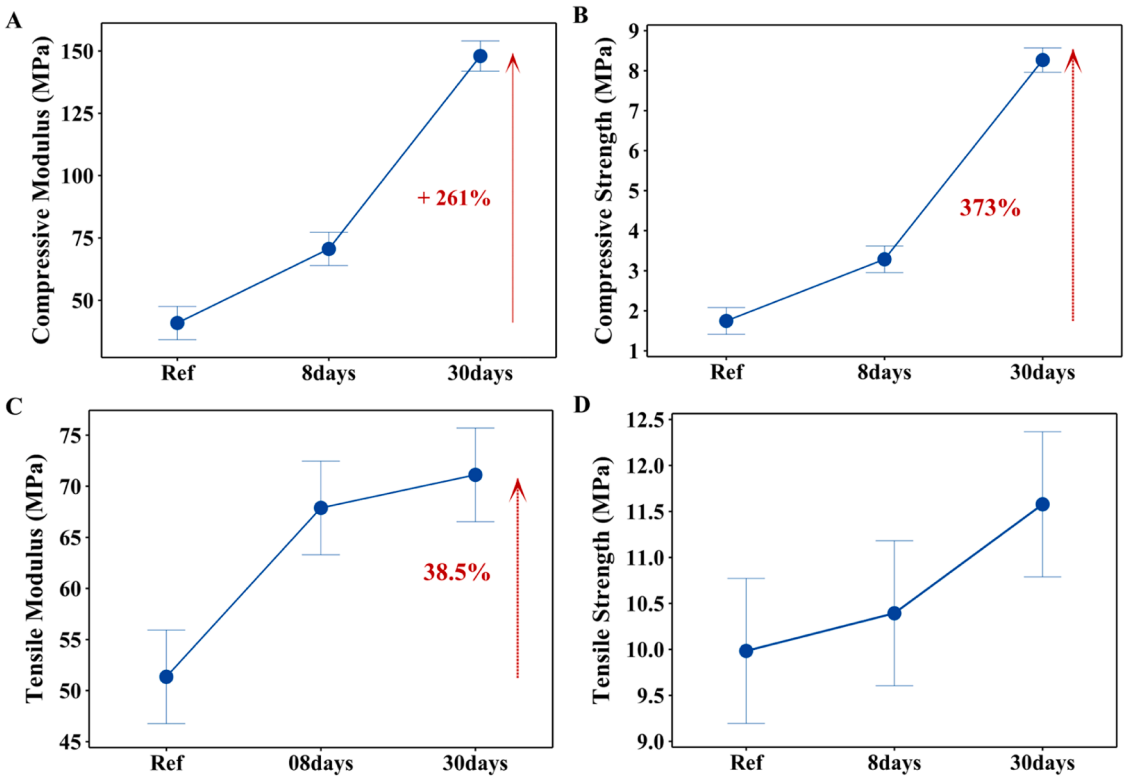

Fig. 6. ANOVA results for compressive (a) modulus and (b) strength; tensile (c) modulus and (d) strength of the biobased polymer.

Table 7
Mean bending properties of sandwich panels.

Core configuration	Time exposure (days)	% RH	Flexural Modulus (GPa)	Core Shear Modulus (MPa)	Maximum Load (N)	Core Shear Stress (MPa)	Facing stress (MPa)
Compacted	8	50	3.4 ± 0.2	32.7 ± 6	1994 ± 133	0.71 ± 0.04	133 ± 8
Compacted	8	100	3.5 ± 0.2	36.4 ± 4	2228 ± 114	0.78 ± 0.05	146 ± 9
Compacted	30	50	3.7 ± 0.3	25.6 ± 6	2224 ± 75	0.78 ± 0.03	147 ± 6
Compacted	30	100	2.7 ± 0.4	19.2 ± 1	1112 ± 218	0.38 ± 0.08	72 ± 14
Spaced	8	50	1.0 ± 0.1	7.1 ± 2	878 ± 180	0.30 ± 0.06	56 ± 11
Spaced	8	100	1.0 ± 0.3	5.6 ± 2	793 ± 64	0.26 ± 0.02	49 ± 4
Spaced	30	50	1.0 ± 0.09	10.6 ± 3	905 ± 90	0.31 ± 0.03	58 ± 5
Spaced	30	100	0.57 ± 0.1	4.6 ± 2	423 ± 106	0.14 ± 0.03	26 ± 6

Table 8
Statistical analysis of the DoE model for the three-point bending properties of the panels.

	Flexural modulus	Core shear modulus	Max. Load	Core stress	Facing stress
$R^{2(adj)}$	96.40 %	92.2 %*	96.32 %	96.50 %	96.50 %
$P\text{-Value}^{AD} \geq 0.05$	0.697	0.260*	0.556	0.704	0.704
$P\text{-Value}^{BvL} \geq 0.05$	0.314	0.535*	0.485	0.504	0.504
$P\text{-Value}^{Core}_{conf.} \leq 0.05$	**0.000**	**0.000**	**0.000**	**0.000**	**0.000**
$P\text{-Value}^{Time}_{exp.} \leq 0.05$	**0.011**	**0.003**	**0.000**	**0.000**	**0.000**
$P\text{-Value}^{\%RH} \leq 0.05$	**0.000**	**0.008**	**0.000**	**0.000**	**0.000**
$P\text{-Value}^{3way\text{-}}_{Int.} \leq 0.05$	0.073	0.851	**0.000**	**0.000**	**0.000**

The observed trend in maximum load-carrying capacity remained consistent for the other response variables. To summarize, the expected effects in a highly aggressive humidity environment led to a reduction of the flexural and core shear modulus properties (Fig. 6c-d), along with a decrease in the resistance capacity of the faces and cores. The statistics presented for the stress in the face skins are similar to those of the core stress (Fig. 6e-f), since both properties were derived from the calculation obtained through the maximum loading. Face skins stress was determined by multiplying a constant (span length divided by twice the face thickness) by the core stress values. This constant factor remained unchanged due to the consistent geometry employed in the sandwich samples. Consequently, core stress was consistently multiplied by this fixed constant value, resulting in identical outcomes in the Design of Experiments (DoE) analysis (Table 8). The subsequent discussion now focuses on the probable deformation mechanisms related to the experimental factors addressed in this research.

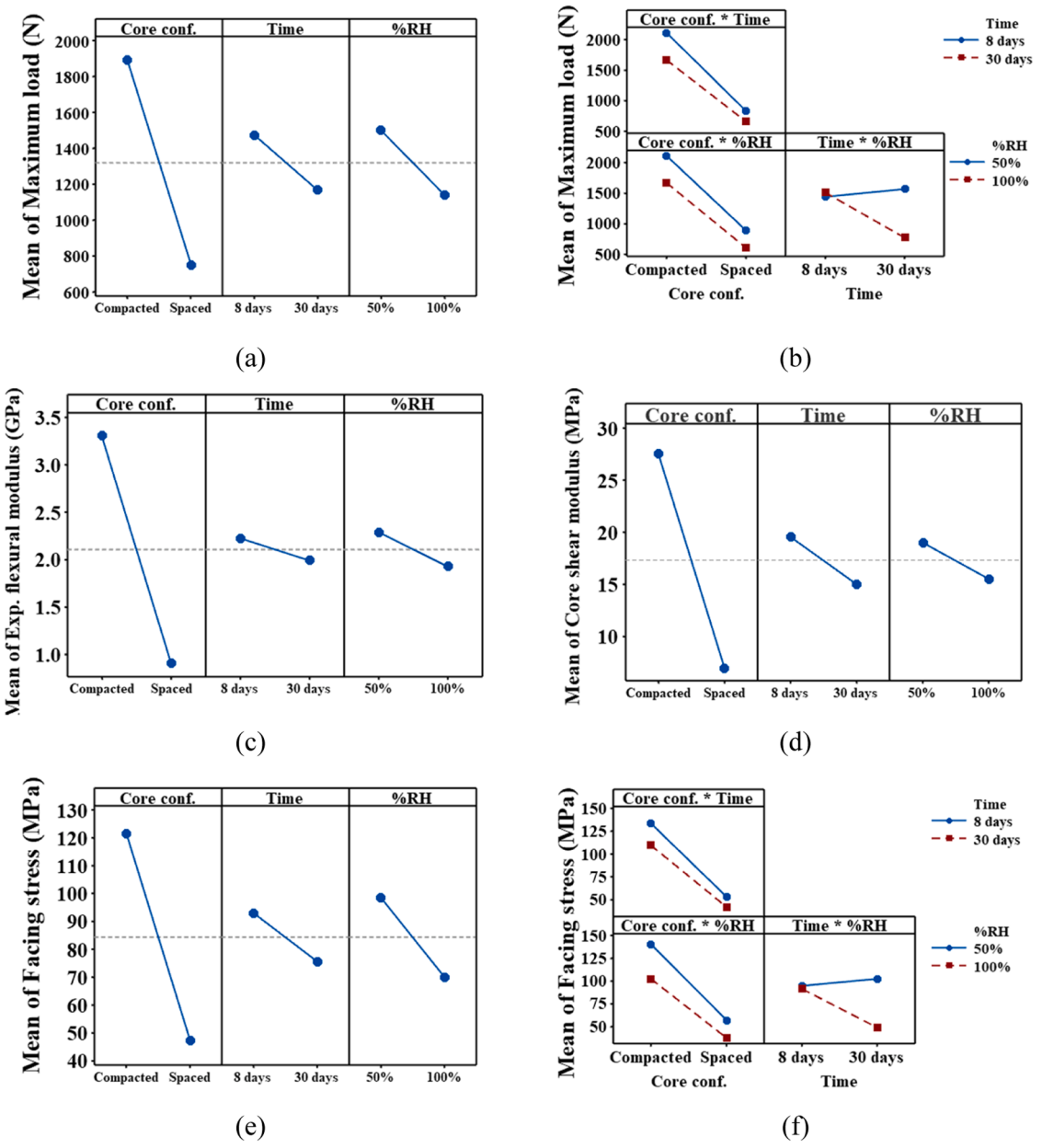

Fig. 7. Plots for main (a) and interaction effects (b) for maximum load; main effect for flexural (c) and core shear modulus (d); and, main (e) and interaction effects (f) for facing stress.

3.5. *Failure mode and the interaction effects of the panel's components*

Fig. 8 displays the typical load-displacement curves for compacted and spaced sandwich panels under pristine (50 % RH, R.T.) and aged conditions (100 % RH, 30 days). Significant decreases in the bending performance of the panels were observed after 30 days of exposure at 100 % RH, particularly for the compacted core samples. Notably, the spaced-core panels experienced a reduction in loading capacity after ageing, but an increase in total displacement, attributed to different failure stages detailed in Fig. 9 and explored below.

The bamboo sandwich panels exhibited high rigidity and were subjected to axial loads during three-point bending tests. This means that the core was responsible for supporting the maximum shear load in the neutral axis, and the maximum axial tensile and compressive load in the lower and upper beam peripheries, respectively. The high rigidity of the core led to an overload of axial loads on its peripheries, impacting the adhesive and the faces, particularly the upper face, which was subjected

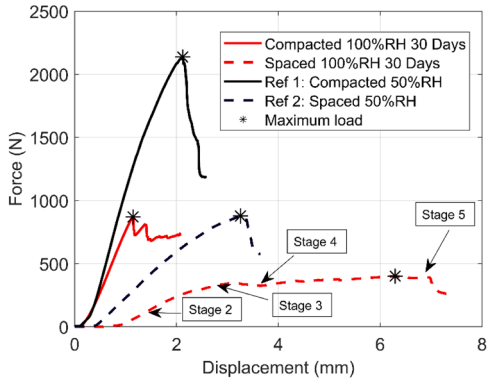

Fig. 8. Typical load-displacement curves for compacted and spaced sandwich panels in pristine (50 % RH, R.T.) and aged conditions (100 % RH, 30 days).

to compressive stresses during bending. In the scenario of a spaced bamboo core configuration, compressive overloading led to buckling of the upper skin, followed by debonding failure (red circles) and rotational movement that detached the lower skin, compromising the entire structure, as depicted in Fig. 9a-f. This effect was less pronounced in panels constructed with compacted bamboo rings, which exhibited a wrinkling effect of the upper skin followed by its debonding, as shown in Fig. 9g.

When the sandwich panel underwent bending, the flexural load was distributed radially within the core, which was influenced by the number of bamboo rings. With 17 and 23 bamboo rings in the spaced and compacted core configurations, respectively, the bending performance was directly affected by the number of rings, which also determined the adhesive contact area between the core and skins.

The mechanical performance of the castor-oil adhesive improved over time, particularly at 30 days, due to the ageing effect (Table 6), while the bamboo rings experienced a decline (Table 7). The relative humidity had contrasting effects, negatively impacting the bamboo rings and positively affecting the adhesive film. The post-curing process in an ageing environment led to an increase in the elastic modulus of the biobased adhesive, reducing its ability to accommodate deformations between the core and skins. Variations in the bulk density of the bamboo cores may have contributed to the decreased adhesiveness and relative movements between the core, adhesive and skins.

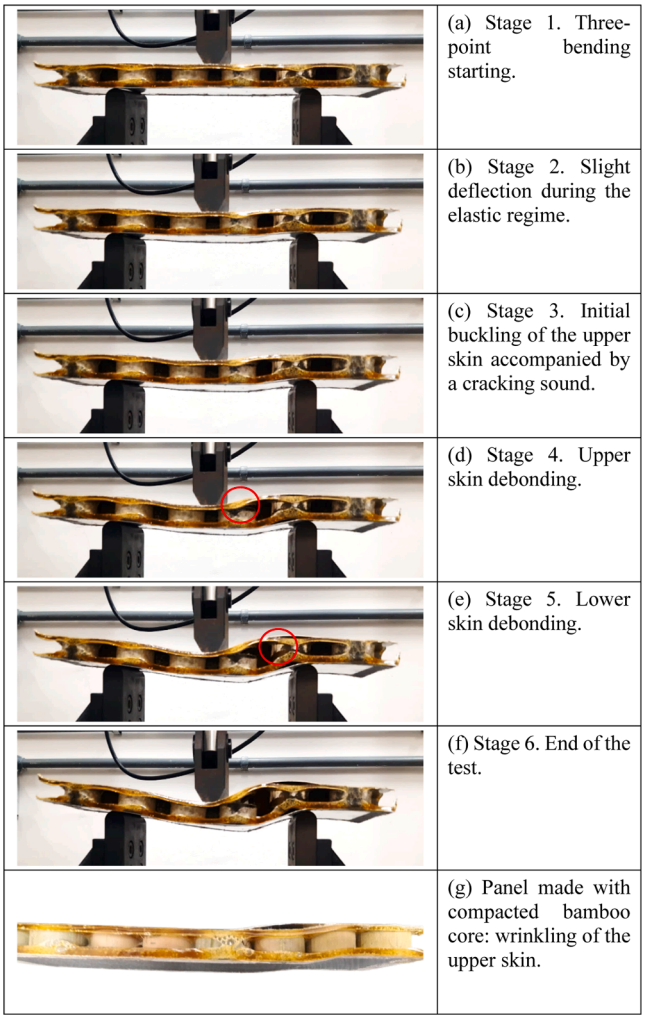

Fig. 9. A typical failure mode evolution through three-point bending of panels made with spaced bamboo core (a-f); and compacted bamboo core (g) under 100 %RH for 30 days.

The decrease in compressive strength of the bamboo rings does not necessarily correspond to a reduction in the bending performance of these bamboo core sandwich materials. The reduction observed in a 100 % humidity chamber could be attributed to a decline in adhesiveness between bamboo rings and the castor oil polymer. Following 8 days under 100 % humidity, the interface between bamboo and castor oil experienced significant water molecule diffusion. This weakened the adhesiveness due to the water molecules, disrupting the primary hydrogen bonds formed during the manufacturing process and leading to a new water-castor oil interaction. As the castor oil polymer became more rigid, its deflection was affected, making the polymer more brittle and unable to sustain a high deformation rate crucial for ensuring better interconnectivity between both faces.

The decrease in bonding within a 100 % humidity chamber can be ascribed to three primary factors: water absorption by the adhesive, hydrolysis of the polyurethane and interference in intermolecular bonds. Water absorption caused adhesive swelling, inducing internal stresses and weakening of the adhesive layer. Additionally, water can permeate the interface between the cured polymer and the bamboo ring surface through microscopic defects or imperfections in the adhesive layer. Capillary action can further aid the entry of water along the interface, worsening the degradation process. Furthermore, water vapour can condense on the substrate surface, providing a continuous supply of moisture that penetrates the polymer, promoting the hydrolysis and swelling processes. Hydrolysis occurs at the interface between the polyurethane (PU) and the bamboo walls. Water molecules break down the polymer chains of the PU at this interface, leading to a reduction in interfacial bond strength and, consequently, a loss of mechanical strength in the sandwich structures. Moreover, the presence of water disrupts the primary hydrogen bonds formed during the manufacturing process, leading to a new water-polymer interaction that diminishes the adhesive's overall performance (Ashcroft and Comyn, 2011; Bowditch, 1996; Ferguson and Qu (2007); Galvez et al. 2019; Kotanen et al. 2021; Tang et al. 2013).

4. Conclusion

We studied the mechanical behaviour of sandwich structures with aluminum skins, featuring a core made of bamboo rings and bio-based adhesive after moisture ageing. Individual characterisation of the bamboo rings revealed that their bulk density initially increased temporarily during the first 8 days of ageing due to swelling from water adsorption, followed by a reduction in saturation after 30 days attributed to the loss of organic material. The bamboo rings exhibited an increase in compressive modulus and strength compared to the reference after 1 or 2 years of natural ageing, which we attributed to the lignification of the bamboo fibres over time. Exposure of the bamboo rings to 100 % relative humidity for 30 days resulted in significant reductions in compressive properties. The castor-oil polymer adhesive was mechanically characterised after wet ageing exposure, showing that its tensile and compressive characteristics improved over time due to the interaction of the water crosslinking agent with the isocyanate groups.

The sandwich panels were tested under two core configurations and humidity levels. The structures composed of hexagonally compacted bamboo rings demonstrated superior maximum flexural load, flexural modulus, core shear modulus, core shear stress and facing stress compared to the spaced core panels. However, the sandwich panels exhibited reduced bending properties after 30 days under 100 % relative humidity conditions. Aged panels with spaced bamboo rings showed wrinkling, followed by skin-core debonding in both skins, while aged panels with compacted cores displayed upper skin buckling and debonding. Future investigations will focus on identifying changes in the chemical composition of bamboo after aging, utilizing NMR spectroscopy at both room temperature and elevated temperatures.

CRediT authorship contribution statement

Fabrizio Scarpa: Writing – review & editing, Conceptualization. **Tulio Panzera:** Writing – review & editing, Supervision, Resources, Conceptualization. **José Ricardo Tarpani:** Supervision, Conceptualization. **Guilherme Germano Braga:** Writing – original draft, Investigation. **Rodrigo José da Silva:** Writing – review & editing, Writing – original draft, Formal analysis. **Júlio Cesar dos Santos:** Writing – original draft, Visualization, Validation, Methodology, Investigation, Formal analysis, Data curation, Conceptualization. **Flávio Napolitano:** Writing – original draft, Investigation, Data curation.

Declaration of Competing Interest

The authors declare the following financial interests/personal relationships which may be considered as potential competing interests. Tulio Hallak Panzera reports financial support was provided by National Council for Scientific and Technological Development. Julio Cesar dos Santos reports financial support was provided by University of São Paulo. Fabrizio Scarpa reports financial support was provided by European Research Council. Flavio Napolitano reports equipment, drugs, or supplies was provided by Imperveg. Tulio Hallak Panzera has patent #BR 10 2020 001263 0 pending to Pending. If there are other authors, they declare that they have no known competing financial interests or personal relationships that could have appeared to influence the work reported in this paper.

Acknowledgements

The authors acknowledge the support of the Brazilian Research Agencies, including CNPq (PQ- 305553/2023–2), USP - Provost of Inclusion and Belonging (PRIP-001/2023, P.N:2023–764) and the European Research Council (ERC-2020-AdG 101020715 NEUROMETA) for the financial support provided. The authors would like to extend their thanks to Imperveg® (Brazil) for providing the castor oil polymer.

Data availability

Data will be made available on request.

References

Ashcroft, I.A., Comyn, J., 2011. Effect of Water and Mechanical Stress on Durability. In: da Silva, L.F.M., Öchsner, A., Adams, R.D. (Eds.), Handbook of Adhesion Technology. Springer, Berlin, Heidelberg. https://doi.org/10.1007/978-3-642-01169-6_31.

Assarar, M., Scida, D., El Mahi, A., Poilâne, C., Ayad, R., 2011. Influence of water ageing on mechanical properties and damage events of two reinforced composite materials: Flax–fibres and glass–fibres. Mater. Des. 32 (2), 788–795. https://doi.org/10.1016/j.matdes.2010.07.024.

Assis, E.G., et al., 2023. Water aging effects on the flexural properties of fully biobased coir fiber composites. Polym. Eng. Sci. https://doi.org/10.1002/pen.26479.

ASTM C393 (2020). Standard Test Method for Core Shear Properties of Sandwich Constructions by Beam Flexure. ASTM International, West Conshohocken/USA.

ASTM D 638 -15 (2015). Standard Test Method for Tensile Properties of Plastics, ASTM International, West Conshohocken/USA.

ASTM D695 – 15 (2015). Standard Test Method for Compressive Properties of Rigid Plastics, ASTM International, West Conshohocken/USA.

ASTM E8/E8M-15a (2015). Standard Test Method for Tension Testing of Metallic Materials. ASTM International, West Conshohocken/USA.

Bitzer, T., 1997. Honeycomb Technology. Springer Netherlands, Dordrecht. https://doi.org/10.1007/978-94-011-5856-5.

Bowditch, M.R., 1996. The durability of adhesive joints in the presence of water. Int. J. Adhes. Adhes. 16 (2), 73–79. https://doi.org/10.1016/0143-7496(96)00001-2.

Cabrera, N.O., Alcock, B., Peijs, T., 2008. Design and manufacture of all-PP sandwich panels based on co-extruded polypropylene tapes. Compos. Part B: Eng. 39 (7–8), 1183–1195. https://doi.org/10.1016/j.compositesb.2008.03.010.

Cai, S., Liu, L., Zhang, P., Li, C., Cheng, Y., 2020. Dynamic response of sandwich panels with multi-layered aluminium foam/UHMWPE laminate cores under air blast loading. Int. J. Impact Eng. 138, 103475. https://doi.org/10.1016/j.ijimpeng.2019.103475.

Castanié, B., et al., 2023. Wood and Plywood as eco-materials for sustainable mobility: a review. Compos. Struct., 117790 https://doi.org/10.1016/j.compstruct.2023.117790.

Chung, J., Waas, A.M., 2000. The in-plane elastic properties of circular cell and elliptical cell honeycombs. Acta Mech. 144 (1–2), 29–42. https://doi.org/10.1007/bf01181826.

Climate Data website, Accessed on June 2024 at ⟨https://pt.climate-data.org/america-do-sul/brasil/minas-gerais/sao-joao-del-rei-25029/⟩.

Daniel, I.M., Ishai, O., 2005. Engineering. Mechanics of Composite Materials. Oxford University press, New York.

de Oliveira, L.A., Passaia Tonatto, M.L., Cota Coura, G.L., Teixeira Santos Freire, R., Hallak Panzera, T., Scarpa, F., 2021. Experimental and numerical assessment of sustainable bamboo core sandwich panels under low-velocity impact. Constr. Build. Mater. 292, 123437. https://doi.org/10.1016/j.conbuildmat.2021.123437.

dos Santos, J.C., et al., 2024. Sandwich structures of aluminium skins and egg-box-shaped cores made with biobased foam and composites. J. Build. Eng. 88, 109099. https://doi.org/10.1016/j.jobe.2024.109099.

dos Santos, A.C., Gatti Cardoso, F., José da Silva, R., de Fátima Gorgulho, H., Hallak Panzera, T., 2022. Modification of short sugarcane bagasse fibres for application in cementitious composites: A statistical approach to mechanical and physical properties. Constr. Build. Mater. 353, 129072. https://doi.org/10.1016/j.conbuildmat.2022.129072.

Dursun, T., Soutis, C., 2014. Recent developments in advanced aircraft aluminium alloys. Mater. Des. (1980-2015) 56, 862–871. https://doi.org/10.1016/j.matdes.2013.12.002.

Ferguson, T.P., Qu, J., 2007. The Effect of Moisture on the Adhesion and Fracture of Interfaces in Microelectronic Packaging. In: Suhir, E., Lee, Y.C., Wong, C.P. (Eds.), Micro- and Opto-Electronic Materials and Structures: Physics, Mechanics, Design, Reliability, Packaging. Springer, Boston, MA. https://doi.org/10.1007/0-387-32989-7_37.

Galvez, P., Abenojar, J., Martinez, M.A., 2019. Effect of moisture and temperature on the thermal and mechanical properties of a ductile epoxy adhesive for use in steel structures reinforced with CFRP. Compos. Part B: Eng. 176 (1)), 107194. https://doi.org/10.1016/j.compositesb.2019.107194.

Gotkhindi, T.P., Simha, K.R.Y., 2015. In-plane effective shear modulus of generalized circular honeycomb structures and bundled tubes in a diamond array structure. Int. J. Mech. Sci. 101–102, 292–308. https://doi.org/10.1016/j.ijmecsci.2015.08.009.

Hartoni, J., Fajrin, B., Anshari, Catur, A.D., 2017. Effect of Core and Skin Thicknesses of Bamboo Sandwich Composite on Bending Strength. Int. J. Mech. Eng. Tech. 8, 551–560. ⟨http://iaeme.com/Home/issue/IJMET?Volume=8&Issue=12⟩.

Heinrich, L.A., 2019. Future opportunities for bio-based adhesives – advantages beyond renewability. Green. Chem. 21 (8), 1866–1888. https://doi.org/10.1039/c8gc03746a.

Hu, L.L., He, X.L., Wu, G.P., Yu, T.X., 2015. Dynamic crushing of the circular-celled honeycombs under out-of-plane impact. Int. J. Impact Eng. 75, 150–161. https://doi.org/10.1016/j.ijimpeng.2014.08.008.

Jakovljević, S., et al., 2017. The influence of humidity on mechanical properties of bamboo for bicycles. Constr. Build. Mater. 150, 35–48. https://doi.org/10.1016/j.conbuildmat.2017.05.189.

Jamil, A., Guan, Z.W., Cantwell, W.J., Zhang, X.F., Langdon, G.S., Wang, Q.Y., 2019. Blast response of aluminium/thermoplastic polyurethane sandwich panels – experimental work and numerical analysis. Int. J. Impact Eng. 127, 31–40. https://doi.org/10.1016/j.ijimpeng.2019.01.003.

Jen, Y.-M., Chang, L.-Y., 2009. Effect of thickness of face sheet on the bending fatigue strength of aluminum honeycomb sandwich beams. Eng. Fail. Anal. 16 (4), 1282–1293. https://doi.org/10.1016/j.engfailanal.2008.08.004.

Jia, H., et al., 2023. Visual evaluation of warehousing humidity and time on bamboo performance. Ind. Crops Prod. 194, 116334. https://doi.org/10.1016/j.indcrop.2023.116334.

Kieling, A.C., et al., 2023. Epoxy-based hybrid composites reinforced with Amazonian Tucumã endocarp and kaolin: A statistical approach to mechanical properties. Materialia 30, 101808. https://doi.org/10.1016/j.mtla.2023.101808.

Kotanen, S., Poikelispää, M., Efimov, A., Harjunalanen, T., Mills, C., Laaksonen, L., Sarlin, E., 2021. Hydrolytic stability of polyurethane/polyhydroxyurethane hybrid adhesives. Int. J. Adhes. Adhes. 110, 102950. https://doi.org/10.1016/j.ijadhadh.2021.102950.

Labans, E., Zudrags, K., Kalnins, K., 2017. Structural Performance of Wood Based Sandwich Panels in Four Point Bending. Procedia Eng. 2017 172, 628–633. https://doi.org/10.1016/j.proeng.2017.02.073.

Lin, T.-C., Chen, T.-J., Huang, J.-S., 2012. In-plane elastic constants and strengths of circular cell honeycombs. Compos. Sci. Technol. 72 (12), 1380–1386. https://doi.org/10.1016/j.compscitech.2012.05.009.

Lopes, da Silva, et al., 2023. Statistical evaluation of three-point bending properties of sustainable aluminium sandwich panels with arched-core geometry. Proc. Inst. Mech. Eng., Part L: J. Mater.: Des. Appl. https://doi.org/10.1177/14644207231219647.

Maria, E., Sarmento, S., Oliveira, W., Silva, R.F., 2007. Moisture Effect on Degradation of Jute/Glass Hybrid Composites. J. Reinf. Plast. Compos. 26 (2), 219–233. https://doi.org/10.1177/0731684407070030.

Napolitano, F., et al., 2023. Sandwich panels made of aluminium skins and gapped-bamboo ring core. J. Braz. Soc. Mech. Sci. Eng. 45 (5). https://doi.org/10.1007/s40430-023-04140-x.

Oliveira, L.A., et al., 2021. Sustainable Sandwich Panels Made of Aluminium Skins and Bamboo Rings. Mater. Res. 24 (4). https://doi.org/10.1590/1980-5373-MR-2020-0543.

Oliveira, P.R., Bonaccorsi, A.M.S., Panzera, T.H., Christoforo, A.L., Scarpa, F., 2017. Sustainable sandwich composite structures made from aluminium sheets and disposed bottle caps. Thin-Walled Struct. 120, 38–45. https://doi.org/10.1016/j.tws.2017.08.013.

Oliveira, P.R., May, M., Panzera, T.H., Hiermaier, S., 2022. Bio-based/green sandwich structures: A review. Thin-Walled Struct. 177, 109426. https://doi.org/10.1016/j.tws.2022.109426.

Oliveira, P.R., Panzera, T.H., Freire, R.T., Scarpa, F., 2018. Sustainable sandwich structures made from bottle caps core and aluminium skins: A statistical approach. Thin-Walled Struct. 130, 362–371. https://doi.org/10.1016/j.tws.2018.06.003.

Oruganti, R.K., Ghosh, A.K., 2008. FEM analysis of transverse creep in honeycomb structures. Acta Mater. 56 (4), 726–735. https://doi.org/10.1016/j.actamat.2007.10.019.

Pizzi, A., Mittal, K.L., 2003. Handb. Adhes. Technol., Revis. Expand. https://doi.org/10.1201/9780203912225.

Regazzi, A., Léger, R., Corn, S., Ienny, P., 2016. Modeling of hydrothermal aging of short flax fiber reinforced composites. Compos. Part A: Appl. Sci. Manuf. 90, 559–566. https://doi.org/10.1016/j.compositesa.2016.08.011.

Santos, J.C., et al., 2020. Ageing of autoclaved epoxy/flax composites: Effects on water absorption, porosity and flexural behaviour. Compos. Part B: Eng. 202, 108380. https://doi.org/10.1016/j.compositesb.2020.108380.

Sheasby, P.G. and Pinner, R., 2001. The Surface Treatment and Finishing of Aluminium and Its Alloys. 6th Edition.

Sun, G., Huo, X., Chen, D., Li, Q., 2017. Experimental and numerical study on honeycomb sandwich panels under bending and in-panel compression. Mater. Des. 133, 154–168. https://doi.org/10.1016/j.matdes.2017.07.057.

Szycher, M., 2012. Structure–Property Relations in Polyurethanes from: Szycher's Handbook of Polyurethanes. CRC Press, pp. 75–77.

Tang, Q., He, J., Yang, R., Ai, Q., 2013. Study of the synthesis and bonding properties of reactive hot-melt polyurethane adhesive. J. Appl. Polym. Sci. 128 (3), 2152–2161. https://doi.org/10.1002/app.38415.

Vial, E.D., et al., 2023. Glass and Aramid Fibre-reinforced Bio-based Polymer Composites Manufactured By Vacuum Infusion: A Statistical Approach to Their Physical and Mechanical Properties. Appl. Compos. Mater. https://doi.org/10.1007/s10443-023-10142-8.

Vieira, L.M.G., Dobah, Y., dos Santos, J.C., Panzera, T.H., Campos Rubio, J.C., Scarpa, F., 2022. Impact Properties of Novel Natural Fibre Metal Laminated Composite Materials. Appl. Sci. 12, 1869. https://doi.org/10.3390/app12041869.

Waddar, S., Pitchaimani, J., Doddamani, M., Barbero, E., 2019. Buckling and vibration behaviour of syntactic foam core sandwich beam with natural fiber composite facings under axial compressive loads. Compos. Part B: Eng. 175, 107133. https://doi.org/10.1016/j.compositesb.2019.107133.

Wang, Z., Li, Z., Xiong, W., 2019. Experimental investigation on bending behavior of honeycomb sandwich panel with ceramic tile face-sheet. Compos. Part B 164, 280–286. https://doi.org/10.1016/j.compositesb.2018.10.077.

Wei, P., Chen, J., Zhang, Y., Pu, L., 2021. Wood-based sandwich panels: a review. Wood Res. 66, 875–890. https://doi.org/10.37763/wr.1336-4561/66.5.875890.

Yuan, J., Chen, Q., Fei, B., 2021b. Investigation of the water vapor sorption behavior of bamboo fibers with different sizes. Eur. J. Wood Wood Prod. https://doi.org/10.1007/s00107-020-01652-4.

Yuan, J., Fang, C., Chen, Q., Fei, B., 2021a. Observing bamboo dimensional change caused by humidity. Constr. Build. Mater. 309, 124988. https://doi.org/10.1016/j.conbuildmat.2021.124988.